ISSN 0965-545X, Polymer Science, Ser. A, 2011, Vol. 53, No. 7, pp. 558–568. © Pleiades Publishing, Ltd., 2011.
Original Russian Text © M.A. Baten'kin, A.N. Konev, S.N. Mensov, S.A. Chesnokov, 2011, published in Vysokomolekulyarnye Soedineniya, Ser. A, 2011, Vol. 53, No. 7, pp. 1033–1043.

Formation of Heterogeneous Polymer Structures During Photoinduced Crosslinking of Oligo(ester acrylates) in the Presence of a Nonpolymerizable Component[1]

M. A. Baten'kin[a], A. N. Konev[a], S. N. Mensov[b], and S. A. Chesnokov[a]

[a] *Razuvaev Institute of Organometallic Chemistry, Russian Academy of Sciences, ul. Tropinina 49, Nizhni Novgorod, 603950 Russia*
[b] *Nizhni Novgorod State University, pr. Gagarina 23, Nizhni Novgorod, 603950 Russia*
e-mail: mensov@ioms.ras.ru

Received September 2, 2010;
Revised Manuscript Received January 27, 2011

Abstract—The morphology of polymers prepared through the photoinduced polymerization of oligo(carbonate dimethacrylate) in the presence of different nonpolymerizable additives (methanol, dinonyl phthalate, hexane, toluene, benzene, and carbon tetrachloride) is studied via the method of atomic force microscopy. Depending on the nature and concentration of an additive, the photoinduced polymerization of the above composite systems is shown to be accompanied by microphase separation and formation of a porous polymeric material. In the case of methanol, homogeneous porous structures with characteristic pore sizes of several hundred nanometers are formed. In the case of dinonyl phthalate, the characteristic pore sizes lie below 100 nm. The synthesized porous polymers can sorb both polar and nonpolar solvents. The photoinduced polymerization of an oligomer in the medium of toluene, benzene, or carbon tetrachloride leads to the formation of polymer nanoparticles whose dimensions are controlled by the nature of a solvent.

DOI: 10.1134/S0965545X11070029

INTRODUCTION

The structurization in a polymer formed owing to crosslinking of dimethacrylates has not yet been investigated in detail. Of special interest is the study of the morphology of polymers produced by the polymerization of oligomers in the presence of various solvents and other nonpolymerizable components. Any cocktail of liquid acrylic oligomers always contains these compounds because of the specific features of their synthesis and the limited potential of distillation for their purification [1]. Moreover, such additives in the form of amines can serve as coinitiating agents of polymerization [2]. Additional introduction of various solvents and plasticizing agents makes it possible to change the viscosity of mixtures and to control the rate and conversion of polymerization and the characteristics of the resultant polymer [3, 4]. If the initial feed composition is a true solution of an oligomer and a neutral additive and the resultant three-dimensional polymer is incompatible with this solution, polymerization can entail phase separation in the system. At high polymerization rates, an inert component cannot be expelled to the boundaries of the polymer sample and phase separation occurs within the polymer bulk. Then, at low concentrations of a nonpolymerizable component, when curing of the system leads to formation of a crosslinked polymer, microphase separation can provide formation of microcavities filled with an inert additive, i.e., formation of a porous polymer. By analogy, at high concentrations of the nonpolymerizable component, individual polymer particles can be formed. The scale of microphase separation depends on diffusion processes occurring in the volume of the system during its crosslinking. For example, for composite systems with a characteristic diffusion coefficient of approximately 1 $\mu m^2/s$ [5] and a polymerization duration of about 1 h, this scale should not exceed tens of microns. However, the duration of photoinduced polymerization is much shorter, and microphase separation should occur at the nanoscale level. In the case of low-molecular-mass additives, for example, methanol [6], at low concentrations (below 10 wt %), microphase separation does not occur and an optically homogeneous polymer forms. These composite materials are used for optical data recording of 3D and patterned polymeric holograms [6–8]. At the same time, there are some publications in which the free-radical copolymerization of several monomers in the presence of an inert component (a pore-forming agent) has been

[1] This work was supported by the Russian Foundation for Basic Research (project nos. 09-03-00668-a, 09-03-12286-ofi_m, and 08-03-97055-r_povolzh'e_a), by a grant from the president of the Russian Federation (NSH-7065.2010.3), and by the federal target program Scientific and Educational Specialists of Innovation Russia (GK P2491).

discussed [9–12]. For example, depending on polymerization conditions, the copolymerization of acrylamide and *N*,*N*'-methylene-bis(acrylamide) in deionized water leads to formation of a porous material with pore sizes ranging from 1 to 100 μm [10]. For macroporous materials based on 2-cyanoethyl methacrylate, 2-hydroxyethyl methacrylate, and ethylene glycol dimethacrylate, pore sizes can range from 0.1 to 1.5 μm [11]. In the case of copolymerization of methyl methacrylate and sodium methacrylate in the presence of poly(ethylene glycol), spherical pores approximately 0.5 μm in size are formed [12]. Porous materials can be effectively used in liquid and gas chromatography [13] as microreactors for the development of inorganic nanoparticles [14] and preparation of bioanalytical microchips [11]. However, materials prepared through the copolymerization of monomers are not always resistant to aggressive media, thus reducing the scope of their practical application. The use of oligo(ester acrylates) makes it possible to solve this problem, because their crosslinking leads to the formation of three-dimensional network polymers that are stable against acids and alkalis and nearly insoluble in organic solvents [1].

This study presents the results of experimental studies of the morphology of heterogeneous polymer structures formed during crosslinking of photopolymerizable systems (PPSs) based on oligo(carbonate dimethacrylate) in the presence of various nonpolymerizable components (dinonyl phthalate (DNP), methanol, hexane, toluene, benzene, and carbon tetrachloride) in a wide concentration range. In addition, the sorptional characteristics of the synthesized porous polymers were studied.

EXPERIMENTAL

Oligo(carbonate dimethacrylate) α,ω-bis(methacryloyloxyethyleneoxycarbonyloxy)ethyleneoxyethylene (OCM-2) (Reper-NN) was used without any additional purification. According to the HPLC data (a Knauer GPC), the content of admixtures (toluene) in the initial OCM-2 sample was 0.4%. Solvents (methanol, hexane, benzene, carbon tetrachloride, and toluene) were purified according to the known procedures [15]. Dinonyl phthalate of the high-purity grade was used as received.

PPCs were prepared via dissolution of an initiating agent in a mixture based on OCM-2 and a nonpolymerizable component. To study pore formation, methanol, DNP, and hexane were used as nonpolymerizable additives. For the preparation of individual polymer particles, the reaction was performed in toluene, benzene, or carbon tetrachloride. A photoinitiating system based on substituted *o*-benzoquinone (0.05 wt %) and *N*,*N*-dimethylethanolamine (1 wt %), which allowed polymerization under optical irradiation in the visible range [2], was used.

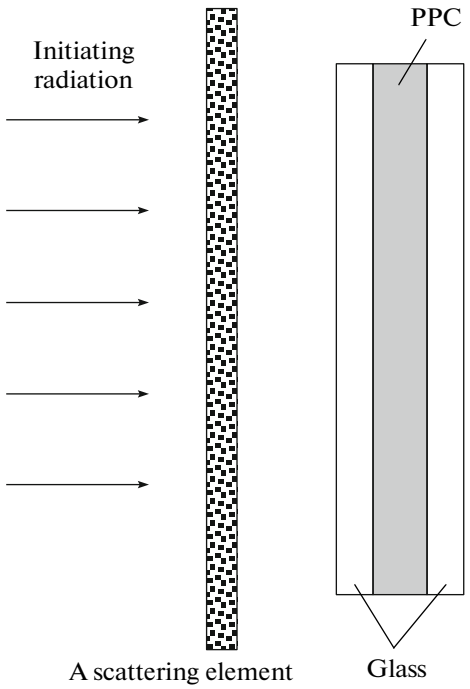

Fig. 1. Scheme of polymerization of PPC and preparation of the porous material.

Polymer samples were prepared as follows. PPC was placed into a mold composed of two pieces of silicate glass with a 2-mm-thick damping piece between them (Fig. 1). To prevent optical amplification of macroscopic density fluctuations in the polymerization system during photoinduced polymerization under directed irradiation [16], initiation was performed with scattered polychromatic light. To study the effect of the nature and concentration of the additive on the morphology of the polymer samples, the illumination was set at 30 klx; the time of polymerization was 60 min. The concentration of the additive was varied from 5 to 50 wt % for methanol and dinonyl phthalate and from 2 to 9 wt % for hexane. Methanol and hexane were removed from the finished polymer sample via evacuation during heating to 60°C. Dinonyl phthalate was removed for the finished polymer sample, via washing with isopropanol, and the isopropanol was evacuated at 60°C.

To study the effect of the intensity of the initiating radiation on the morphology of the formed polymer, illumination was varied from 10 to 50 klx. In the experiments, the radiation dose was fixed, whereas the exposure time was varied from 180 to 35 min, respectively. In this case, methanol (30 wt %) was used as a nonpolymerizable component.

For the preparation of individual polymer particles, the concentration of the oligomer in the PPC was 5 wt %. The system was polymerized in a degassed ampoule under the effect of scattered polychromatic light with an illumination of 100 klx for 1 h under con-

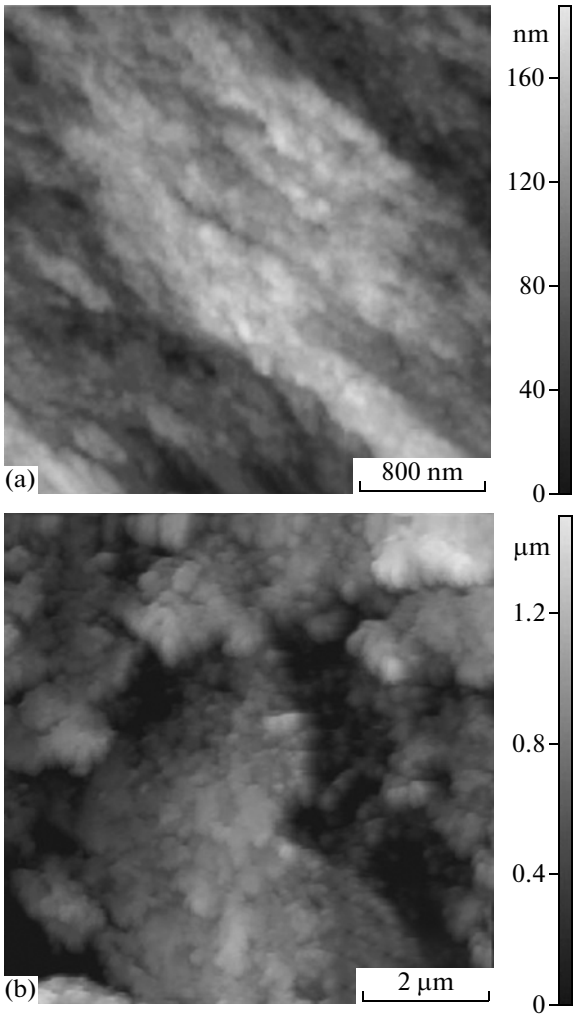

Fig. 2. AFM image of the fractured surface of the polymer synthesized from PPC containing (a) 5 and (b) 30 wt % methanol.

stant stirring. The precipitate formed during photoinduced polymerization in toluene and benzene was deposited onto a glass support, and the residual solvent was evacuated at 60°C. When polymerization proceeded in the medium of carbon tetrachloride, the formed precipitate was deposited onto a glass support via dipping and the residual solvent was evaporated in air.

The resultant polymer samples (monolithic, porous, and individual particles) were analyzed on NT-MDT Smena-A and Solver R47 microscopes. The samples were scanned in the tapping mode. To study the bulk structure of the polymer samples, the samples fractured. Both the fractured surface of the samples and the surface of the polymer samples contacting the reactor glass were examined. In this case, the scale of analyzed objects was varied from tens of nanometers to tens of microns. The characteristic sizes of heterogeneities in the polymer structures were estimated from the autocorrelation function of the spatial distribution of the surface relief obtained in AFM observations as the half-width of the autocorrelation function. In addition, the surface morphology of the polymer synthesized from the PPC containing 10 wt % DNP was examined on a Supra 50VP scanning electron microscope (SEM).

The existence of pores in the polymer samples produced in the presence of additives was verified by sorption in various liquids at room temperature (20°C), and the maximum sorptional capacity was estimated. As sorbates, both polar and nonpolar solvents were used: water and benzene. The maximum sorptional capacity was defined as the capacity at which the content of the sorbed component in a sorbent remained constant for 1 day.

RESULTS AND DISCUSSION

AFM Studies of the Polymer Samples Prepared via Photopolymerization of Oligo(ester acrylate) in the Presence of Nonpolymerizable Components

The polymerization of dimethacrylic oligomers, including OCM-2, proceeds under gel-effect conditions, even at its early stages, when conversion is ~1–3% [1]. This process is accompanied by the hardening (monolithization) of the initial liquid system and the development of microheterogeneities in the bulk of the polymerizing material under certain conditions. In the case of the photoinduced polymerization of OCM-2 in the presence of inert ethylene glycol dimethacrylate (10 wt %) under similar conditions, the gel effect arises within 3–5 min after the onset of irradiation. The limiting conversion is 65% and is achieved within 80 min after the onset of irradiation with an illumination of 10 klx [17].

The photoinduced polymerization of OCM-2 in the presence of 50 wt % methanol under the conditions described in Experimental leads to formation of solid polymer samples. As a result of the photoinduced polymerization of the composite systems containing less than 15 wt % methanol, monolithic and optically transparent polymer glass is formed. Figure 2a shows the AFM image of the fractured surface of the polymer sample prepared from the PPC containing 5 wt % methanol. The morphology of this polymer is similar to the morphology of the polymer prepared via crosslinking of the PPC without any admixtures [16] and appears as a globular structure; the globules are several tens of nanometers in size [18]. In addition, the surface of these samples (contacting the reactor glass) is optically homogeneous. It is possible to distinguish globules less than 50 nm in size, and the height of surface relief does not exceed 15 nm (Fig. 3a).

When the concentration of methanol in the initial PPC is 15–25 wt %, the polymer structure in the bulk of the sample is similar to that of the sample for which the methanol content is below 15 wt %; that is, in its

bulk, the polymer material is optically homogeneous. However, its surface is coated with a white patina. The AFM observations showed that the surface of the polymer sample prepared from the PPC containing 20 wt % methanol includes large-scale heterogeneities with lateral sizes exceeding several microns and a height of several hundreds of nanometers (Fig. 2b). A higher resolution AFM image of some surface fragments (Fig. 2b) reveals heterogeneities with lateral sizes of nearly 100 nm. It seems that, during polymerization, methanol is partially expelled from the bulk of the reaction mixture to the surface; hence, its concentration near the surface of the sample becomes higher than the initial concentration, thus promoting microphase separation. When the concentration of methanol exceeds 25 wt %, the reaction mixture becomes opaque as early as within the very first minutes of photoinduced polymerization. It may be expected that, at these concentrations of methanol, polymerization entails the microphase separation of the polymerizing system and the formation of microcavities filled with methanol. Since the refractive indexes of POCM-2 and methanol are substantially different ($n_{\text{OCM-2}} = 1.5030$ and $n_{\text{MeOH}} = 1.3288$), the formed microheterogeneities are capable of effective light scattering. As a result, an optically opaque material is formed.

On the surface of the polymer sample synthesized from the PPC containing 30 wt % methanol, it is possible to observe a well-pronounced heterogeneous structure; the lateral sizes of heterogeneities and the height of the surface relief are several hundred nanometers (Fig. 3c). Similar randomly heterogeneous structures are seen at the fractured surface of this sample along with some other imperfections of the fractured surface, and their characteristic sizes are several microns (Fig. 2b). Note that this range of characteristic sizes of volume heterogeneities and the fractured surface dramatically restrict further interpretation of the collected images. Volume and surface structures have identical morphologies; hence, the AFM images of the surfaces of the polymer samples with volume heterogeneities are presented below and, for each batch of the samples, reference observations of the fractured surfaces were performed.

The polymerization of the PPC in the presence of methanol with a weight content exceeding 30% leads to the formation of a heterogeneous polymer structure, but the heterogeneities are bigger. For example, for the polymer sample synthesized from the PPC containing 35 wt % methanol, the sizes of heterogeneities and the relief height exceed one micron (Fig. 3d). When the content of methanol in the PPC exceeds 50 wt %, a brittle polymer material easily disintegrating into parts is produced.

Figure 4 presents the results of the AFM observations for the samples prepared from PPC containing different amounts of DNP. The heterogeneous polymer is seen to be produced even when the concentration of the additive is 10 wt % (Fig. 4b): The sizes of heterogeneities do not exceed 100 nm, but the relief height is 150 nm. When the content of the neutral component increases, as in the case of methanol, pore dimensions tend to grow. In the AFM image of the surface of the polymer sample synthesized from PPC containing 40 wt % DNP, the morphology is more complicated, the sizes of heterogeneities are below 1 μm, and the relief height is 850 nm (Fig. 4c). Note that the samples with volume heterogeneities become opaque not during photoinduced polymerization but only after removal of the inert additive from the sample. The absence of light scattering during microphase separation of DNP and POCM-2 is related to the closeness of their refractive indexes ($n_{\text{OCM-2}} = 1.5030$ and $n_{\text{DNP}} = 1.487$). At the same time, after the removal of DNP, the released space within the sample is occupied by air ($n_{\text{air}} = 1$) and the difference in refractive indexes becomes significant.

In addition, the surface morphology of the polymer synthesized from PPC containing 10 wt % DNP was examined on a scanning electron microscope (Fig. 5). Since the OCM-2 polymer is a dielectric, its surface can be decorated with a metallic layer with a thickness of ~15 nm via the magnetronic deposition technique. It was found that, under the action of an electron beam, the sample breaks down during SEM observations (Fig. 5a). This fact substantially impedes examination of the POCM-2 samples via the methods of electron microscopy. Nevertheless, we managed to select proper imaging regimes and thus collect fair and well-resolved SEM images; these SEM images make it possible to distinguish characteristic details in the surface topography of the test samples (Fig. 5b). The SEM image (Fig. 5b) visualizes heterogeneities whose structure and dimensions are similar to those identified in the AFM observations (Fig. 4b).

An analysis of polymer structures synthesized from hexane-containing PPC shows that, when the concentration of this solvent does not exceed 2 wt %, a transparent polymer glass forms (Fig. 6a). When the concentration of hexane increases up to 4 wt %, the surfaces of the resultant polymer samples contain singular heterogeneities less than 1 μm in size (Fig. 6b). The sizes of these heterogeneities are less uniform, and their quantity is appreciably smaller than that in the samples prepared in the presence of methanol and DNP. When the concentration of hexane increases up to 9 wt %, the whole pattern illustrating heterogeneities of the polymer structure remains nearly unchanged (Fig. 6c). This result is likely due to the fact that the separation of hexane into an individual phase proceeds at a higher rate than polymerization; hence, the excess solvent is expelled toward the surface of the sample that contacts the glass. When concentrations exceed 9 wt %, the microphase separation of the system occurs long before polymerization.

Figure 7 presents the autocorrelation function of the spatial distribution of the surface relief of polymer

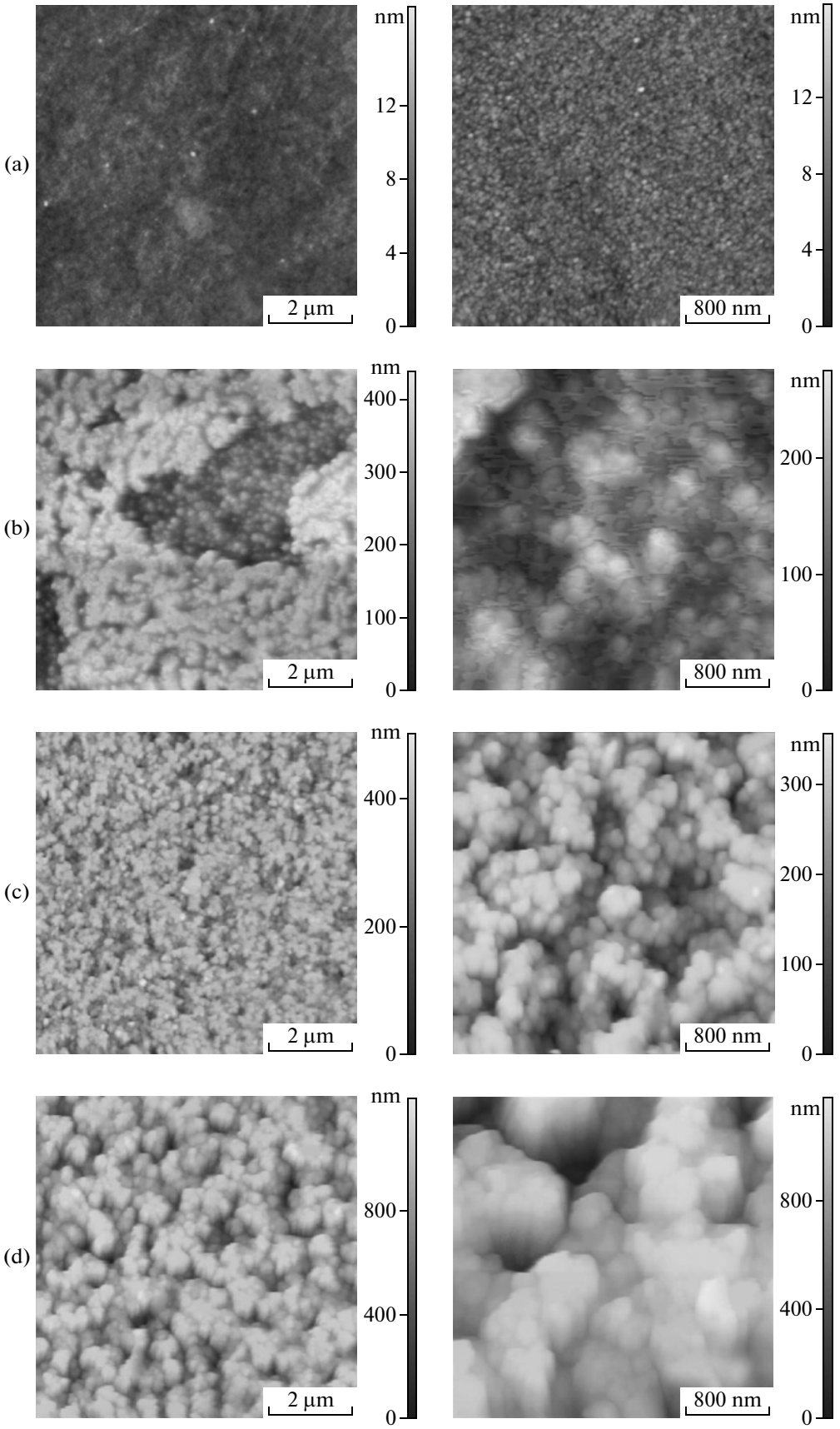

Fig. 3. AFM image of the surface of the polymer synthesized from PPC containing (a) 5, (b) 20, (c) 30, and (d) 35 wt % methanol.

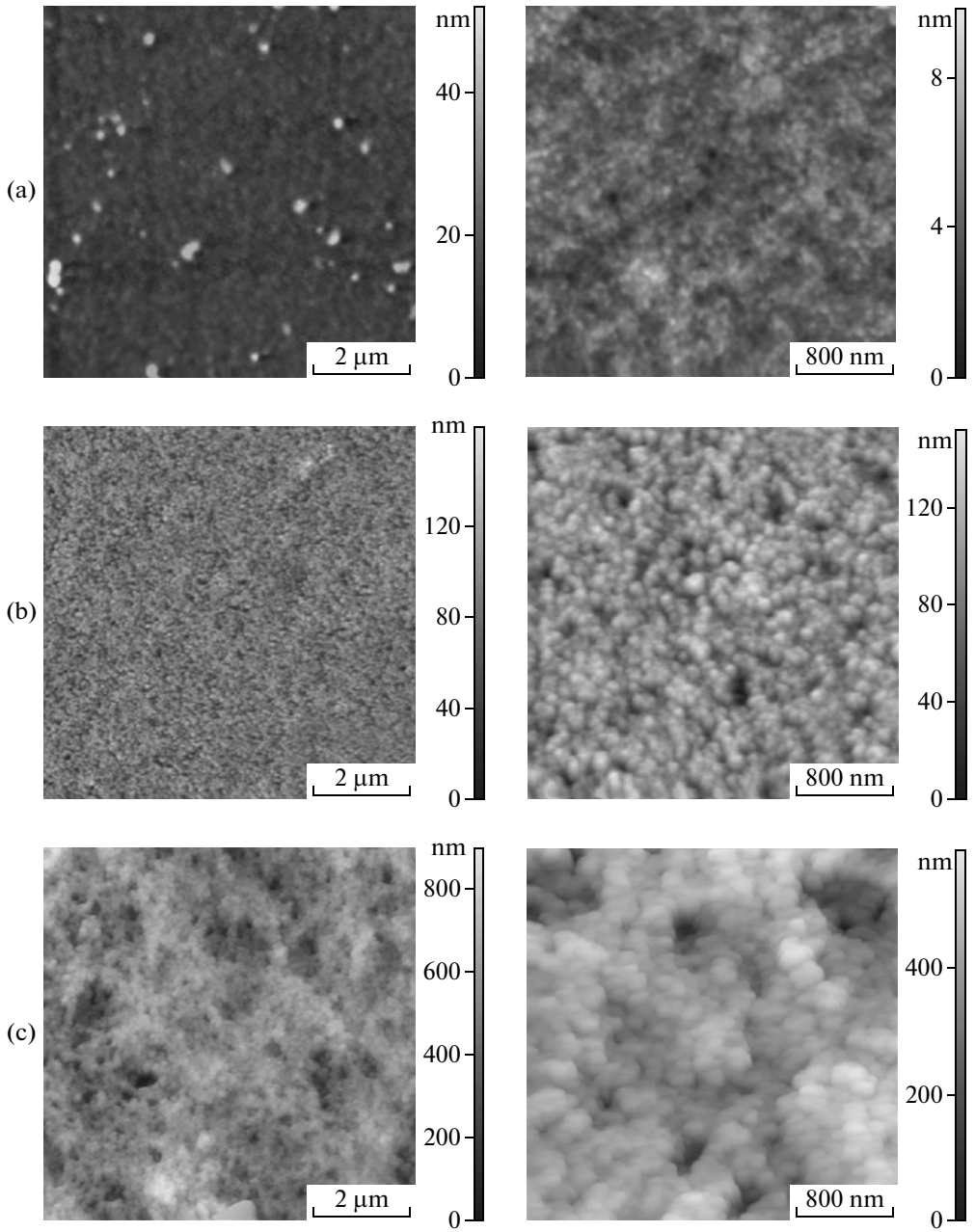

Fig. 4. AFM image of the surface of the polymer synthesized from PPC containing (a) 5, (b) 10, and (c) 40 wt % DNP.

samples prepared in the presence of methanol (30 wt %) and DNP (10 wt %). In the case of methanol, the characteristic sizes of structural heterogeneities in polymers (the half-width of the autocorrelation function) are 200 ± 20 nm (Fig. 7a). For DNP, these heterogeneities are smaller: 60 ± 20 nm (Fig. 7b). It may be expected that a difference in the sizes of the heterogeneities is related to the viscosity of the existing additives. Compared to DNP, methanol has a notably lower viscosity ($\eta_{MeOH} = 5.45 \times 10^{-4}$ mPa s [15], $\eta_{DNP} = 113–123$ mPa s [5]). It seems that methanol is more effectively redistributed in the volume of the reaction mixture during polymerization, and bigger conglomerates form.

Because an increase in the intensity of the initiating light causes an increase in the polymerization rate [4], the effect of the intensity of actinic radiation on the morphology of the formed polymer was studied. As follows from Fig. 8, when the illumination intensity increases from 10 to 20 klx, the characteristic sizes of heterogeneities (the half-width of the autocorrelation function of the spatial distribution of the surface relief) decrease more than two times. When illumination

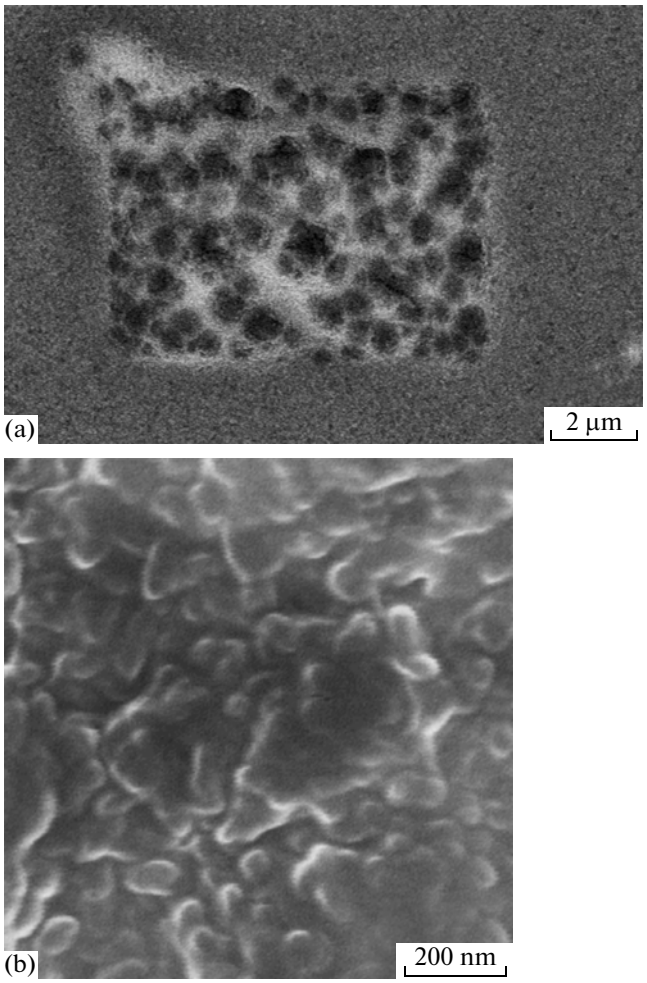

Fig. 5. SEM images of the surface of the polymer synthesized from PPC containing 10 wt % DNP. The images were recorded in secondary electrons with an in-lens detector: (a) degradation of the polymer under the action of the electron beam in the SEM, (b) the SEM micrograph recorded in the safe regime.

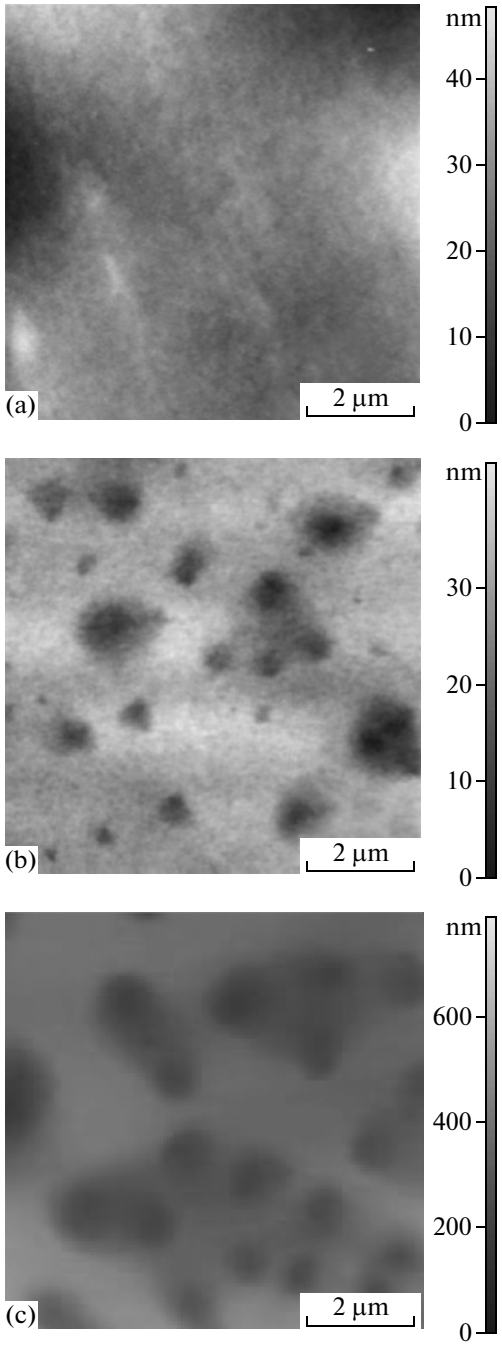

Fig. 6. AFM image of the surface of the polymer sample synthesized from PPC containing (a) 2, (b) 4, and (c) 9 wt % hexane.

increases further, the dimensions of heterogeneities remain practically unchanged.

Therefore, the photoinduced polymerization of OCM-2 in the presence of nonpolymerizable additives, which form true solutions in a wide concentration range, can lead to formation of a monolithic sample and a heterogeneous polymer. This phenomenon can be qualitatively explained by the phase-state diagrams for the oligomer–polymer–nonpolymerizable-additive mixture (Fig. 9) that are constructed on the basis of the following speculations. The oligomer becomes incompatible with its own polymer, at a certain minimum conversion [1]. In the phase diagrams (Fig. 9), this conversion is depicted by straight line *NP**. At low concentrations, the neutral component is compatible with a polymer network; in the diagrams, this concentration is depicted as point *N**. As the concentration of the polymer in the PPC increases (in the course of polymerization), the line corresponding to the boundary of compatibility between a nonpolymerizable additive and a polymer should approach point *N**. When an oligomer and a nonpolymerizable additive are compatible at all ratios, this line commences at point *N* (Fig. 9a, line *NZN**). In the case of limited compatibility, this line should start at point *Z* on the *ON* axis (Fig. 9b, line *ZN**). Point *Z* in Fig. 9b corre-

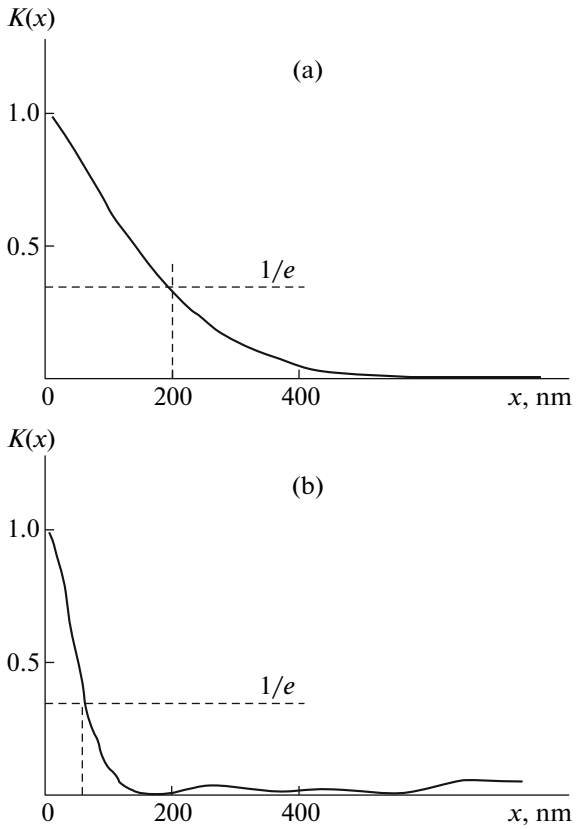

Fig. 7. Autocorrelation functions of the space distribution of the surface relief $K(x)$ for the polymer samples prepared in the presence of (a) 30 wt % methanol and (b) 10 wt % DNP.

sponds to the limiting solubility of a nonpolymerizable additive in the oligomer. The diagrams include the following regions:

(*1*) where there is a homogeneous three-component medium,

(*2*) where a nonpolymerizable additive is compatible with an oligomer and a polymer that are incompatible with each other,

(*3*) where a polymer is incompatible with all other components of the PPC, and

(*4*) where a polymer is compatible with an oligomer but a nonpolymerizable additive is separated into an individual phase.

In the course of the polymerization of PPC containing a low concentration of a nonpolymerizable additive, whose concentration is below N^* (this case corresponds to the movement of an imaging point along straight line *A*), a neutral component is preserved in the polymer network; crosslinking leads to the formation of a transparent monolithic sample. When concentration increases above N^*, polymerization is accompanied by separation of the nonpolymerizable component into an individual phase and by formation of a porous polymer (movement of the imaging point along straight line *B*) or individual polymer particles (straight line *C*).

Sorptional Characteristic of Porous Polymers Synthesized from Oligo(ester acrylate) OCM-2

Pores in the heterogeneous polymer samples formed in the presence of methanol and DNP were studied also in sorption experiments. As sorbed solvents, distilled water and benzene were used. The measure of sorptional capacity S is defined as the ratio of the volume of the solvent sorbed by the polymer to the limiting volume of pores in a sample, which is estimated as the volume of a pore-forming agent in the initial PPC.

Figure 10 presents the sorptional characteristics of the synthesized porous polymers plotted against the concentration of a nonpolymerizable component. For the samples prepared in the presence of methanol (Fig. 10a), the profiles of sorption curves for water and benzene are nearly the same.

When the concentration of methanol is below 20 wt %, the synthesized polymers sorb practically none of the above solvent. When the concentration of methanol is 20–30 wt %, sorption occurs, a result that indicates the formation of an open porous structure in

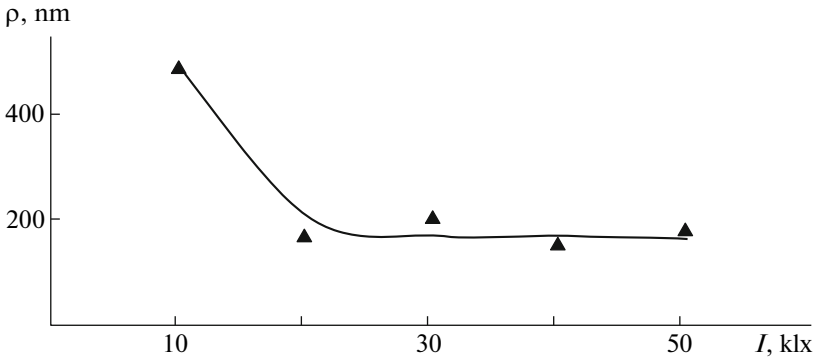

Fig. 8. Characteristic heterogeneity sizes ρ for the polymer samples synthesized from PPC containing 30 wt % methanol plotted against intensity I of the initiating light.

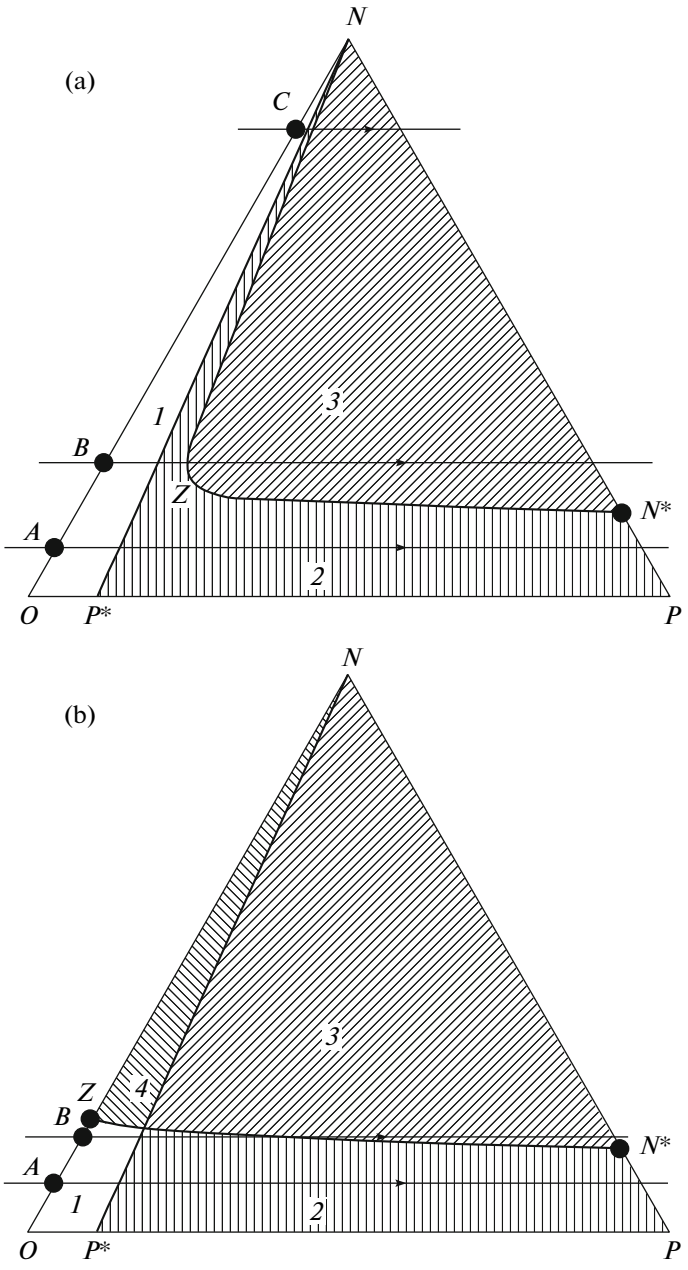

Fig. 9. The expected phase-state diagrams for the oligomer (O)–polymer (P)–nonpolymerizable-component (N) three-component system: (a) the oligomer and the neutral component are compatible at all ratios and (b) the oligomer and the neutral component are partially compatible.

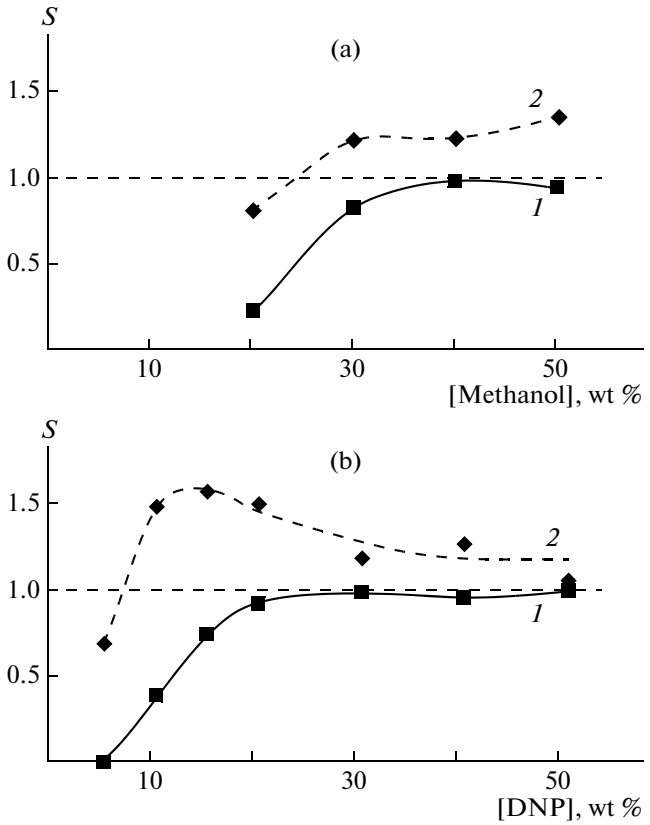

Fig. 10. Ratios of the volumes of (*1*) water and (*2*) benzene absorbed by the polymer to the limiting volume of pores in the samples, *S*, plotted against solvent concentration: (a) the polymer prepared in the presence of methanol and (b) the polymer prepared in the presence of DNP.

the polymer bulk. When the concentration of methanol in the PPC increases further, the ratio between the volume of the sorbed solvent and the limiting volume of pores remains unchanged. The limiting water sorption is approximately unity; i.e., water occupies the whole volume of the pores. In the case of benzene, sorption is higher than unity; this phenomenon may be due to partial swelling of the polymer matrix. When DNP serves as a nonpolymerizable component (Fig. 10b), the sorption curves have similar profiles. The limiting sorption of water approaches unity, while the sorption of benzene exceeds unity. The only difference is that sorption is observed for the samples prepared at lower concentrations of the pore-forming agent (5–10 wt %). This observation agrees with the AFM data (Fig. 4), which show that a heterogeneous polymer is formed even when the content of DNP in the PPC is ~10 wt %. The sorption curve for benzene shows a maximum at DNP concentrations of 10–20 wt %, a result that can be explained as follows. The OCM-2 polymer is known to partially swell in organic solvents [18]. The relative of *S* is calculated with allowance for not only the volume of benzene in the pores of the polymer material but also the volume absorbed by the polymer matrix. As a result, at low concentrations of benzene, *S* is much higher than unity. As the content of the pore-forming agent in the initial composition increases, the volume of pores increases, while the content of benzene sorbed by the polymer network remains unchanged. As a result, *S* decreases and the dependence of *S* on the content of the nonpolymerizable agent in the initial composition approaches the plateau region.

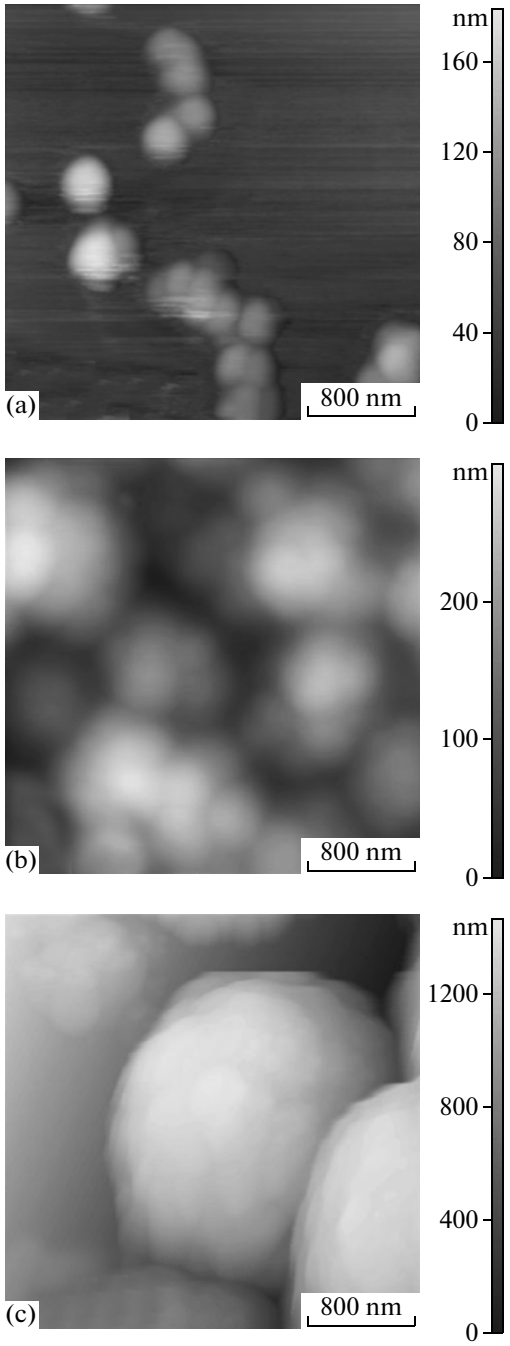

Fig. 11. Polymer nanoparticles formed via polymerization of the OCM-2 oligomer in (a) carbon tetrachloride, (b) toluene, and (c) benzene.

Hence, the prepared porous polymer samples can sorb appreciable amounts of both benzene and water. Therefore, in the bulk of the polymer sample, there is a system of interpenetrating pores whose surface is characterized by nearly the same hydrophobicity and hydrophilicity. Note that, after introduction or removal of the model solvents, the samples themselves do not markedly change.

Photoinduced Polymerization of Oligo(ester acrylate) OCM-2 in Excess Solvent

When an oligomer is cured in the presence of large amounts of a solvent, no one-piece sample can be formed. For example, when the content of methanol or DNP exceeds 50 wt %, polymerization yields a brittle polymer material. Photoinduced polymerization of the oligomer in a solvent should lead to the formation of individual polymer particles (Fig. 9a). This statement has been experimentally verified for carbon tetrachloride, toluene, and benzene. Figure 11 presents the AFM images of the nanoparticles formed via the photoinduced polymerization of oligo(ester acrylate) OCM-2 in the presence of large amounts of various solvents. (The weight fraction of the oligomer is 5 wt %.) The sizes of particles depend on the nature of the solvent in which polymerization is conducted. The sizes of nanoparticles are 200–300 nm in the case of carbon tetrachloride and 400–800 nm in the case of toluene. When polymerization proceeds in benzene, the sizes of the particles are ~2000 nm.

CONCLUSIONS

The photoinduced crosslinking of polymers in the presence of a nonpolymerizable component leads to formation of a polymer material whose morphology and porosity depend on the nature and concentration of the additive as well as on the intensity of the initiating radiation. In the bulk of the polymer sample, the porous structure is formed only in a certain interval of concentrations of the pore-forming agent. Beyond this concentration interval, an optically uniform polymer monolith (at a low content of the additive in the PPC) or individual polymer particles (at a high content of the additive) form. As the viscosity of a nonpolymerizable component and the intensity of initiating radiation increase, pore size tends to decrease. The surfaces of pores show both hydrophilic and hydrophobic characteristics; as a result, the prepared porous materials feature a good sorptional capacity with respect to water and benzene. The polymerization of the oligomer at high concentrations of the solvent can lead to the formation of individual polymer nanoparticles.

ACKNOWLEDGMENTS

We would like to thank S.A. Gusev (Institute for Physics of Microstructures, Russian Academy of Sciences) for SEM studies of the samples.

REFERENCES

1. A. A. Berlin, T. Ya. Kefeli, and G. V. Korolev, *Poly(ester acrylates)* (Nauka, Moscow, 1967) [in Russian].
2. S. A. Chesnokov, V. K. Cherkasov, G. A. Abakumov, et al., Izv. Akad. Nauk, Ser. Khim., No. 12, 258 (2001).
3. A. A. Berlin, *Acrylic Oligomers and Related Materials* (Khimiya, Moscow, 1983) [in Russian].

4. Yu. D. Semchikov, *High Polymers* (Nizhegorodsk. Gos. Univ., Nizhni Novgorod, 2003) [in Russian].
5. *Encyclopedia of Polymers* (Sovetskaya Entsiklopediya, Moscow, 1974), Vol. 2 [in Russian].
6. M. A. Baten'kin, S. N. Mensov, and A. V. Romanov, Opt. Spektrosk. **104**, 149 (2008).
7. G. M. Karpov, V. V. Obukhovskii, and T. N. Smirnova, Opt. Spektrosk. **82**, 145 (1997).
8. M. A. Baten'kin, S. N. Mensov, and A. V. Romanov, Opt. Zh. **75** (5), 34 (2008).
9. T. I. Izaak and O. V. Vodyankina, Usp. Khim. **78**, 80 (2009).
10. F. Plieva, X. Huiting, I. Yu. Galaev, et al., J. Mater. Chem. **16**, 4065 (2006).
11. E. G. Vlakh, E. F. Maksimova, V. D. Krasikov, and T. B. Tennikova, Polymer Science, Ser. B **51**, 327 (2009) [Vysokomol. Soedin., Ser. B **51**, 1677 (2009)].
12. T. I. Izaak, O. V. Babkina, A. N. Salanov, et al., Polymer Science, Ser. A **45**, 560 (2003) [Vysokomol. Soedin., Ser. A **45**, 939 (2003)].
13. A. Yu. Kanat'ev, A. A. Kurganov, E. N. Vikitorova, and A. A. Korolev, Usp. Khim. **77**, 393 (2008).
14. L. M. Bronshtein, S. N. Sidorov, and P. M. Valetskii, Usp. Khim. **73**, 542 (2004).
15. A. J. Gordon and R. A. Ford, *The Chemist's Companion. A Handbook of Practical Data, Techniques and References* (Wiley, New York, 1972; Mir, Moscow, 1976).
16. G. A. Abakumov, M. A. Baten'kin, S. N. Mensov, et al., Materialovedenie, No. 11, 39 (2007).
17. S. A. Chesnokov, V. K. Cherkasov, G. A. Abakumov, et al., Izv. Akad. Nauk, Ser. Khim., No. 12, 2258 (2001).
18. Yu. M. Sivergin, R. Ya. Perkins, and S. M. Kireeva, *Polycarbonate(meth)acrylates* (Zinatne, Riga, 1988) [in Russian].